Approaches to the study of the evanescent field of terahertz surface plasmon polaritons at the Novosibirsk free electron laser

V. Kukotenko, V. Gerasimov

V. D. Kukotenko, V. V. Gerasimov, "Approaches to the study of the evanescent field of terahertz surface plasmon polaritons at the Novosibirsk free electron laser," Proc. SPIE 12776, Infrared, Millimeter-Wave, and Terahertz Technologies X, 1277607 (26 November 2023); doi: 10.1117/12.2687472

Event: SPIE/COS Photonics Asia, 2023, Beijing, China

Approaches to the study of the evanescent field of terahertz surface plasmon polaritons at the Novosibirsk free electron laser

V.D. Kukotenko *[a], V.V. Gerasimov[a,b]
[a]Budker Institute of Nuclear Physics SB RAS; [b]Novosibirsk State University

ABSTRACT

Currently, in photonic integrated circuits, the circuit size is limited by diffraction, which acts as a barrier to further development in the field of optical communications. Plasmonics could potentially address this size mismatch between electronic and photonic components. Photonics and plasmonics can complement each other, given the appropriate conditions, allowing optical signals to be converted into surface plasmon-polaritons (SPPs) and vice versa. Therefore, plasmonic integrated planar circuits for wireless communication devices are actively being developed. Transitioning to the terahertz (THz) frequency range will enhance data transmission and processing speed. In the development of plasmonic integrated circuits, understanding the optical properties of surfaces is crucial. Current methods for determining the optical properties of surfaces in the THz frequency range lack sufficient sensitivity to transitional surface layers of metal and films that are much thinner than the optical wavelength. This work will demonstrate experimental methods for measuring the penetration depth of the SPP field into the air. Through these methods, and utilizing other plasmonic refractometric characteristics, it is possible to reconstruct the effective surface dielectric permittivity of the metal.

Keywords: Terahertz surface plasmons polariton, surface plasmons polariton, Novosibirsk free electron laser, terahertz range, penetration depth, evanescent field, diagnostics of the quality of surfaces.

INTRODUCTION

One of the applications of terahertz surface plasmon-polaritons (SPPs) propagating along the conductor-dielectric interface is waveguide surface refractometry. The conductor can be a metal, dielectric in the absorption band, graphene, or a doped semiconductor. Measuring the SPP characteristics (refractive index, penetration depth of the SPP field into the dielectric) allows for the reconstruction of the optical properties of the conductor, which is important for surface quality diagnostics, thin film analysis, sensing, and more.

This work explores two experimental methods for detecting the penetration depth of the evanescent SPP field into the air: (1) the probe method with external modulation and probe oscillation modulation; (2) the method of "shielding" the surface wave. The measured penetration depths of the SPP field at a wavelength of 141 μm on the "Au-ZnS-air" structure with a zinc sulfide (ZnS) layer thickness of 0.7 μm will be presented.

EXPERIMENTAL SETUP

As a source of radiation in our experiments, we utilized the Novosibirsk Free Electron Laser (NovoFEL), generating a continuous sequence of pulses with a duration of 100 ps, following at a repetition rate of 5.6 MHz. The radiation from NovoFEL is linearly polarized and can be tuned within the ranges of 90–340 μm, 37–80 μm, and 8–11 μm [1]. The NovoFEL beam exhibits complete transverse coherence and a small divergence on the order of 0.2 degrees. The methods for registering the SPP field, described later, can be employed with various radiation sources, including significantly less powerful gas lasers, backward-wave oscillators, and others.

In the experimental setup depicted in Figures 1 and 2, a p-polarized Gaussian beam from NovoFEL with a diameter of 23 mm and a wavelength of 141 μm was used. The average power of the radiation was approximately 10 W, and a wire-grid polarizer was utilized at the input to regulate the power. The intensity of the incident beam was monitored using a polypropylene beam splitter and a pyroelectric sensor.

*V.D.Kukotenko@inp.nsk.su;

Infrared, Millimeter-Wave, and Terahertz Technologies X, edited by Cunlin Zhang,
Yiwen E., Masahiko Tani, Proc. of SPIE Vol. 12776, 1277607 · © 2023 SPIE
0277-786X · doi: 10.1117/12.2687472

Probe method

To generate and detect SPPs using the probe method, an experimental configuration shown in Figure 1 was utilized. The laser beam, reflecting off the alignment mirror 1, illuminated the mirror 2 with a gold coating. Subsequently, the beam was focused onto the edge of the sample 4 using a parabolic mirror 3 with a focal length f = 75 mm. The focused radiation was partially transformed into SPPs due to diffraction, and these SPPs then propagated along the sample surface. The sample had a smooth curvature of 13 degrees to reduce parasitic bulk waves that occurred during diffraction at the edge. For the same reason, a "slit" made of foam with a size of 1 mm was placed at the center of the sample to shield against unwanted illumination. At the other end of the sample, SPPs were scattered by a metallic probe oscillating at a frequency and amplitude set by the periodic sinusoidal signal generator G3-112 (Russia). The scattered radiation was collected by a lens (in a 2f-2f arrangement) with a focal length f = 75 mm and focused on the input aperture of the Golay cell 5.

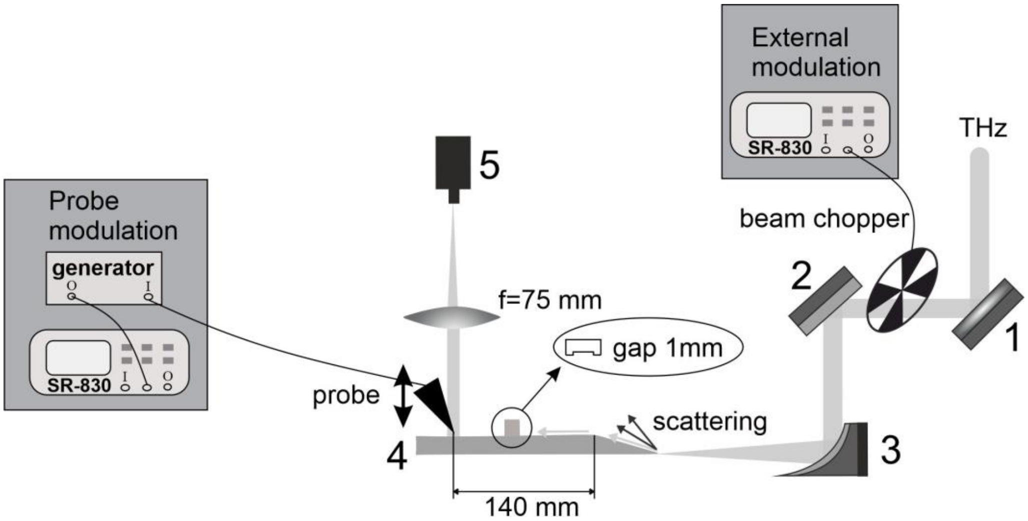

Figure 1 - Installation for detecting surface plasmon polaritons (SPPs) using the probe method.

Two types of modulation were used for radiation detection. The first is the previously mentioned modulation with probe oscillations, created using a generator. The second is external modulation, implemented using a mechanical chopper placed at the entrance of the setup. The Golay cell signal and the synchronous signal with the reference frequency of the generator (or chopper, accordingly) were sent to the synchronous detector SR-830.

Shielding method

The experimental technique depicted in Figure 2 involved recording the intensity of SPPs that passed beneath a metallic screen. To alter the distance z between the sample surface and the screen, the latter was fixed on a translation stage moved along the z-axis. A portion of the SPP energy that did not pass under the screen was scattered from the edge of the screen.

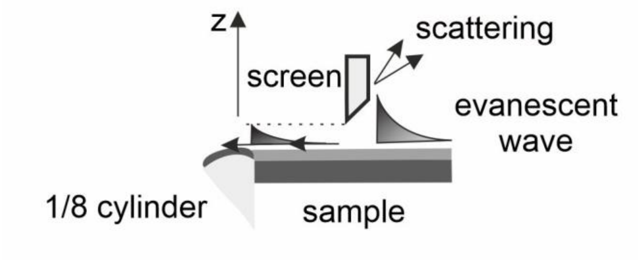

Figure 2 – Schematic representation of part of the installation for detecting SPP using the “shielding” method.

For measuring the evanescent field of SPPs, the setup depicted in Figure 3 was utilized. The laser beam from the NovoFEL, passing through the system of calibration mirrors 1, 2, illuminated a cylindrical metallic mirror with a focal length f = 75 mm. The beam was focused onto the edge of the sample 4. The radiation focused on the sample's edge was partially transformed into SPPs due to diffraction, which then propagated along the sample surface. Next, the beam passed through a vertical slit 5, 1 mm in height, made of a material opaque to THz radiation, used for shielding against unwanted illumination. After the sample, the SPPs propagated along the 1/8 cylinder 6. The cylinder, as shown in Figure 6, was essential to reduce the portion of parasitic waves in the recorded signal by spatially separating the SPPs from the parasitic bulk waves. These bulk waves arose at the input due to diffraction of the radiation focused by mirror 3 on the edge of the sample, as well as due to radiation losses of the SPPs [2]. The diffracted evanescent wave from element 6 was detected by the Golay cell 7.

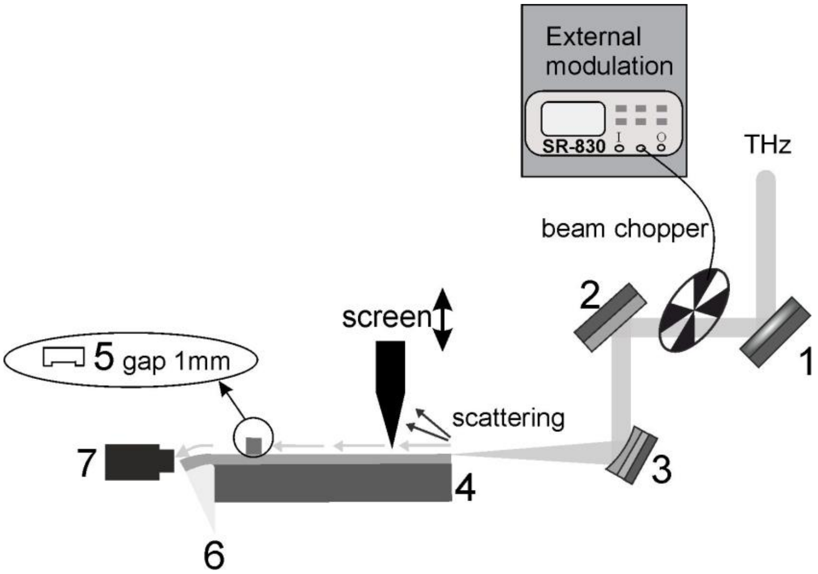

Figure 3 – Installation for detecting SPP using the “shielding” method.

Sample

The structure of the sample, depicted in Figure 4, comprised a flat glass plate with a polished top surface onto which an opaque gold (Au) layer, 300 nm thick, was deposited using magnetron sputtering. Over the gold layer, a layer of zinc sulfide (ZnS) was deposited using electron beam evaporation. The thickness of the ZnS layer was 0.7 µm. The dimensions of the samples were 100x100x11 mm.

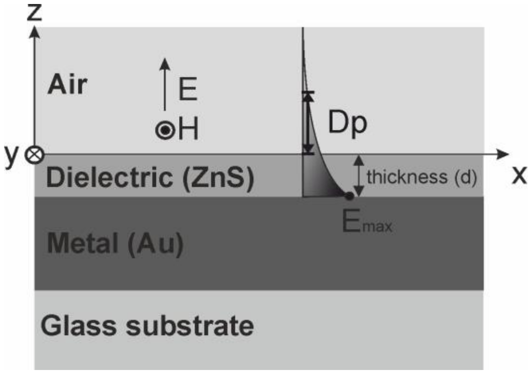

Figure 4 – Schematic representation of the sample structure. x - distance from the edge of the sample, Dp - penetration depth, d - thickness of the ZnS layer, z - distance from the probe to the sample surface, E - electric field strength, H - magnetic field strength.

RESULTS AND DISCUSSION

The dependence of the useful signal from the synchronous detector on the voltage supplied to the probe (see Fig. 1) is presented in Fig. 5.

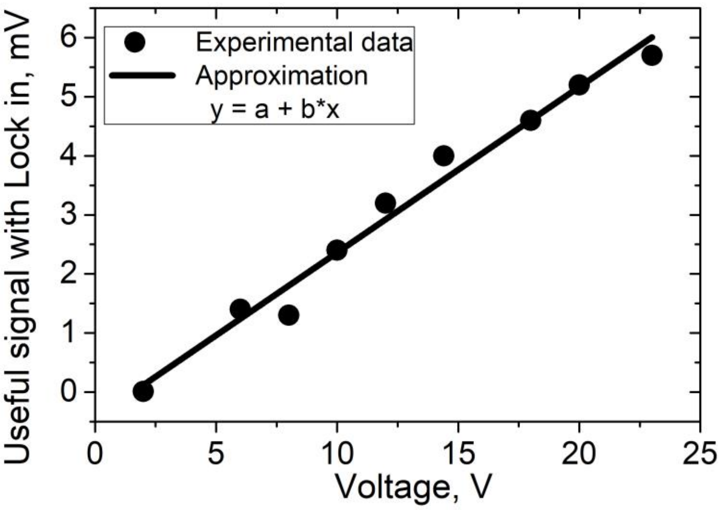

Figure 5 – Dependence of the useful signal on the voltage supplied to the probe. Probe modulation ν=30 Hz was used.

During the experiment, it was observed that at an applied voltage of 23 V, the probe made contact with the surface of the sample. Therefore, the experiment proceeded using the maximum allowable value of 20 V, at which no contact occurred.

For the plots in Figures 6 and 7, noise was subtracted from the useful signal. Based on the results of the exponential fit of the graph in Figure 6, the penetration depth of SPPs into the air (based on intensity) was determined to be dp = 0,482± 0,007 mm.

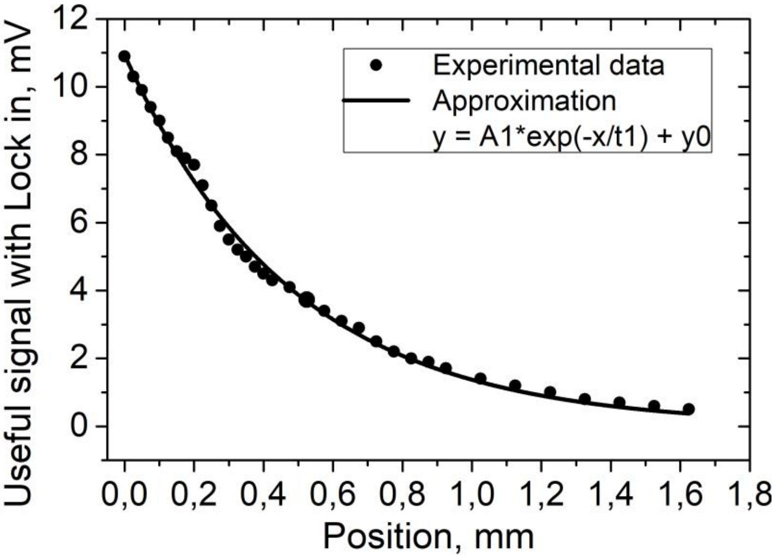

Figure 6 – Dependence of the useful signal on the distance to which the probe is raised from the surface of the sample. External modulation ν=30 Hz was used. Noise level 0.3 mV.

Figure 7 shows measurements with probe vibrations. At the maximum voltage applied to the probe, the dependence of the useful signal from the synchronous detector on distance was measured. The penetration depth was dp = 0,49±0,15 mm.

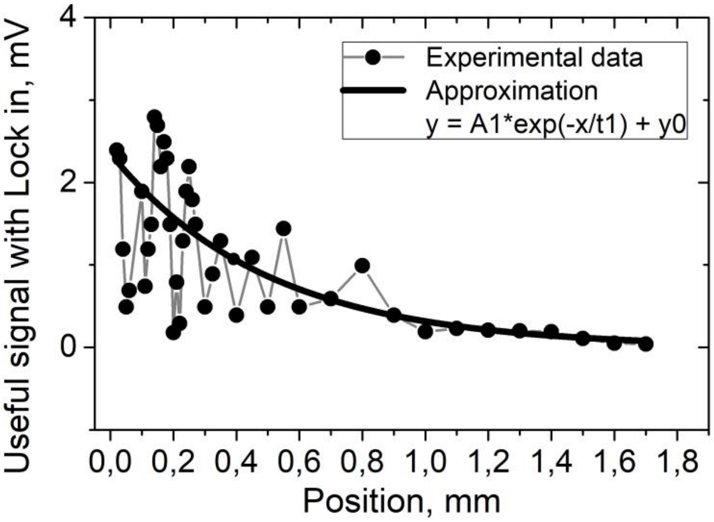

Figure 7 – Dependence of the useful signal on the distance to which the probe is raised from the surface of the sample. Probe modulation was used. Noise level 0.01 mV.

To detect SPPs using the shielding method, the setup depicted in Figures 2 and 3 was employed. Figures 8 and 9 display the experimental data obtained through the shielding method. The relationship between the useful signal from the synchronous detector and the distance between the shield and the sample was obtained. The penetration depth was calculated dp = 0,53±0,14 mm.

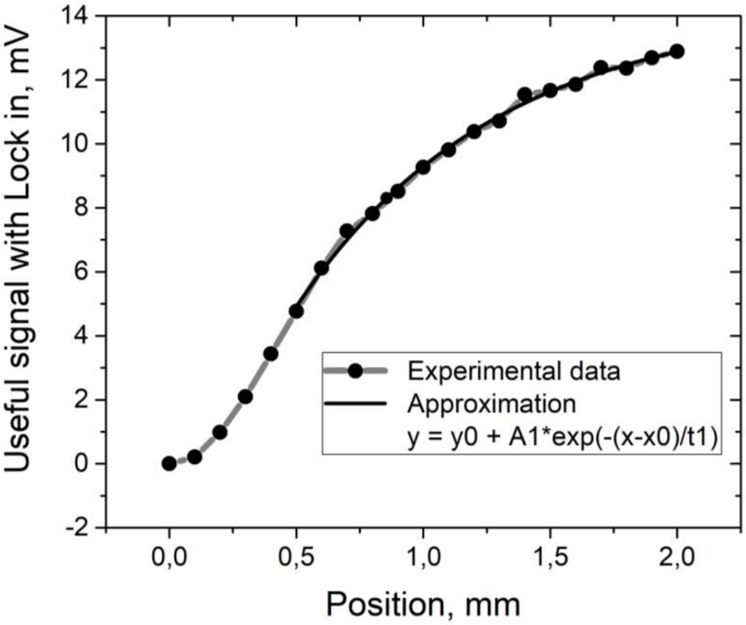

Figure 8 – Dependence of the useful signal on the distance to which the screen rises from the surface of the sample.

If we take the derivative of the experimental dependence in Fig. 8, then we obtain the profile of the decline in the evanescent field of the SPP (Fig. 9). After approximating this dependence, the penetration depth was dp = 0,53±0,14 mm.

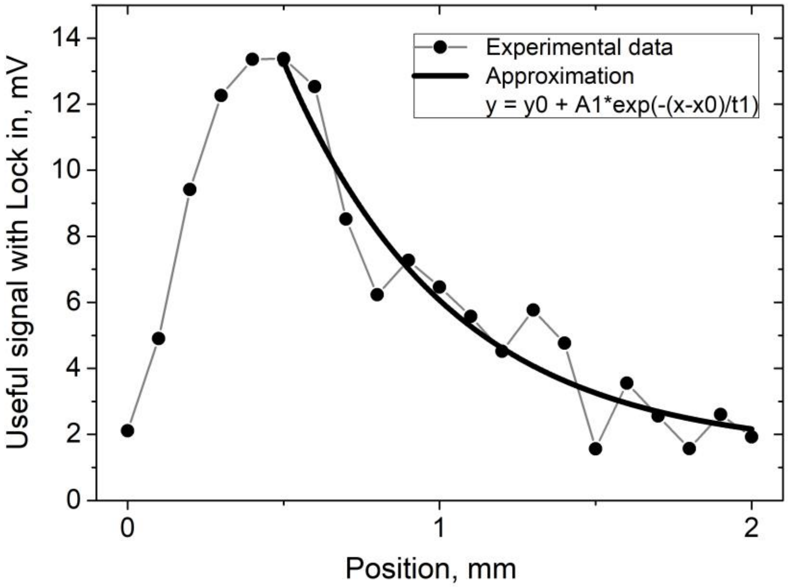

Figure 9 – Dependence of the useful signal on the distance to which the screen rises from the surface of the sample.

Table 1 presents the results of measuring the penetration of the SPP field on the Au-ZnS-air structure using the three methods presented above.

Table 1. Results of test experiments on the "Au-ZnS-air" structure λ = 141 μm.

Measurement technique	**Penetration depth, mm**
Probe method, external modulation	0.482±0.007
Probe method, probe modulation	0.49 ±0.15
Shielding	0,53 ±0,14

CONCLUSION

Experiments on the "Au-ZnS-air" structure measuring the penetration depth of the SPP field into the air using three different methods demonstrated good agreement in depth of penetration within the margin of error. This indicates the reliability of the results and the functionality of all three registration methods. These methods can be utilized for non-destructive testing of the optical constants of conducting surfaces.

ACKNOWLEDGEMENTS

The work was done at the shared research center «Siberian Center for Synchrotron and Terahertz Radiation» on the basis of the Novosibirsk FEL at the Institute of Nuclear Physics SB RAS.

REFERENCES

[1] Bolotin V.P., Vinokurov N.A., Kayran D.A. et al. // Nucl. Instrum. and Methods. Phys. Res. 2005. V. A543. P. 81.; O. A. Shevchenko, N. A. Vinokurov, V. S. Arbuzov, et al., The Novosibirsk free electron laser facility, AIP Conference Procee dings 2299, 020001 ,pp. 020001-1 — 020001-8, (2020). https://doi.org/10.1063/5.0031513

[2] V. Gerasimov, B. Knyazev, Growth of terahertz surface plasmon propagation length due to thin-layer dielectric coating, Journal of Optical Society of America B. V. 33, Is. 11, P. 2196-2203 (2016).